ARTICLE IN PRESS

Citrus flavanones mildly interfere with pituitary-thyroid axis in old-aged male rats

Marko Miler [a,*], Ivana Jarić [a], Jasmina Živanović [a], Vladimir Ajdžanović [a], Nasta Tanić [b], Verica Milošević [a], Branka Šošić-Jurjević [a]

[a] Department of Cytology, Institute for Biological Research "Siniša Stanković", University of Belgrade, Belgrade, Serbia
[b] Department of Radiobiology and Molecular Genetics, Institute of Nuclear Sciences "Vinča", University of Belgrade, Belgrade, Serbia

ARTICLE INFO

ABSTRACT

Citrus flavanones naringenin (NAR) and hesperetin (HES) are potent antioxidants that may contribute to maintenance of health at old age by improving cardiovascular and metabolic status. However, they may also affect thyroid hormone economy. Keeping in mind impaired thyroid function at older age, in this study we tested wheather NAR or HES administration potentiate this decline. NAR or HES were administrated orally (15 mg/kg) to male 24-month-old Wistar rats during 4 weeks. Control groups received vehicle, sunflower oil. Qualitative and quantitative immunohistochemical and immunofluorescent expression of specific proteins and stereological analyses of thyroid tissue were performed. Thyroid stimulating hormone (TSH) and total thyroxine (T_4) concentrations were measured in serum. Thyroid parenchyma of both flavanone-treated groups was characterized by lower ($p < 0.05$) absolute and relative volume of luminal colloid, accompanied by elevated ($p < 0.05$) relative volume of stroma in comparison with the controls. No hypertrophy or absolute thyroid volume change was detected. Intensity of immunopositive signal for thyroglobulin (Tg) and T_4 bound to Tg (T_4-Tg) increased ($p < 0.05$) in the colloid of thyroid follicles after both flavanone treatments. Serum TSH increased ($p < 0.05$) after NAR, while T_4 remained unchanged after both treatments. In conclusion, NAR elevated serum TSH in old-aged males, thus being more potent than HES in altering pituitary-thyroid axis. However, changes in thyroid structure, namely moderate colloid depletion and higher Tg and T_4-Tg protein expressions after both treatments, indicate preserved capacity of the gland to compensate flavanone interfering, and maintain T_4 production in old-aged males.

© 2017 Elsevier GmbH. All rights reserved.

1. Introduction

Aging is a complex process characterized by a progressive decline in cellular function, overall health and well-being, as well as increased risk of age-related diseases and death. Alterations of the endocrine system and the induction of age-related endocrine diseases significantly contribute to disturbed cellular and molecular metabolic control (Bowers et al., 2013; Chahal and Drake, 2007; Vitale et al., 2013).

Hypothyroidism is very common in patients over 60 years of age and steadily increases with age. The prevalence of thyroid autoimmune diseases and carcinoma increases with advanced age in both sexes (Morganti et al., 2005; Kim et al., 2010; Boelaert 2013). However, according to more recent studies, healthy elderly and centenarians have higher serum thyroid stimulating hormone (TSH) concentrations than younger individuals (Atzmon et al., 2009; Surks and Hollowell, 2007). In male rats, aging is characterized by lower serum thyroid hormone (TH) levels, along with unchanged serum and pituitary TSH level (Cizza et al., 1995; Reymond et al., 1992). Increased number of triiodothyronine (T_3) receptors and deiodinase enzyme (Dio) type 2 activity has been reported in the pituitary of aged male rats (Donda et al., 1990) indicative of adaptation to hypothyroid or hypothyroxinemic alterations.

Citrus flavanones, naringenin (NAR) and hesperetin (HES) are bioactive compounds found mostly in grapefruit and orange fruits (Erlund, 2004). Their consumption has been associated with healthy aging and prevention of cardiovascular diseases, metabolic dysfunction and osteoporosis (Cavia-Saiz et al., 2010; Chanet et al., 2012; Galluzzo et al., 2008). Due to their phenolic structures, these flavanones are good blocators (scavenger) of reactive oxygen species (ROS) (Cavia-Saiz et al., 2010). We showed improved antioxidant status and phospholipid composition in the liver of old-aged male rats upon both flavanone treatments, NAR being more potent than HES (Miler et al., 2016).

Besides andtioxidant, flavonoids display diverse biological and pharmacological properties, including antithyroid effects in experimental animals and humans. Namely, NAR was reported to inhibit thyroid peroxidase in vitro (TPO; Divi and Doerge, 1996) and 5′-deiodinase in vivo (Cody et al., 1986), the key enzymes of TH synthesis and metabolism. Administration of high doses of NAR and HES glycoside precursors (naringin and hesperidin) decreased serum concentration of thyroxine (T_4) and T_3 in hyperthyroid rats (Panda and Kar 2014). However, the intensity of antithyroid effect of polyphenols vary, and depend on animals' diet, dose, age and/or pathological state (Chang and Doerge, 2000; Schmutzler et al., 2004; Šošić-Jurjević et al., 2014).

To the best of our knowledge, there are no data regarding thyroid structure and its functional status in 24-month-old rats after administration of citrus flavanones. In this study we tested if NAR or HES, administered at nutritional doses interfere with pituitary-thyroid axis and potentiate the natural decline of thyroid functioning in our old-aged model.

2. Materials and methods

2.1. Animals and experimental groups

Male Wistar rats (24-month-old) were housed in the unit for experimental animals at the Institute for Biological Research "Siniša Stanković", Belgrade, Serbia. All animals had free access to standard food (Veterinarski zavod, Subotica, Serbia) and water, and were maintained at constant temperature ($21 \pm 2\,°C$) and lighting (12 h light: 12 h dark) conditions.

At the beginning of the experiment, the rats were randomly divided in four experimental groups (n = 6 for each group). One group of animals received per os (p.o.) 15 mg/kg b.w. of NAR, while the other was treated in a same way with HES (Sigma Aldrich, St. Louise, MO, USA).The citrus flavanones were mixed with sunflower oil (Vital, Vrbas, Serbia), the applied volume of mixture was 0.3 ml per animal and the way of application was by syringe directly to the oral cavity. Control group (CON) received the same volume of the vehicle, while old-aged intact controls (ICON) did not receive any treatment. The treatments were administrated daily for 4 weeks.

The animals were decapitated without anesthesia; their thyroid glands including part of the trachea were excised, fixed in 4% paraformaldehyde solution for 24 h and dehydrated in increasing concentrations of ethanol (30–100%) and enlightened in xylene. After embedding in Histowax (Histolab Product Ab, Göteborg, Sweden), each tissue block was serially sectioned at 5 μm thickness on a rotary microtome (RM 2125RT Leica Microsystems, Wetzlar, Germany).

All animal procedures were in compliance with Directive 2010/63/EU on the protection of animals used for experimental and other scientific purposes, and was approved by the Ethical Committee for the Use of Laboratory Animals of the Institute for Biological Research "Siniša Stanković", University of Belgrade (No 2-12/12).

2.2. Histochemical staining procedures

Thyroid sections were stained by routine haematoxylin and eosin (H&E) and Masson trichrome technique for the qualitative and quantitative histological analyses. Masson trichrome staining was applied to get insight into the connective tissue distribution (Ajdžanović et al., 2017). In brief, deparaffinised and rehydrated thyroid sections were incubated in Weigherts' haematoxylin, following acid fuchsine and Ponceau mixture for 5 min, phosphomolybdenum acid for 10 min and aniline blue for 4 min, respectively. In between, the slides were washed in tap or distilled water. Sections were dehydrated and mounted in DPX (Sigma-Aldrich, Barcelona, Spain). All digital images of the thyroid sections regarding light microscopy were made on a DM RB Photomicroscope (Leica, Wetzlar, Germany) with a DFC 320 CCD Camera (Leica) for the images acquisition and analysis.

2.3. Stereological analyses

We performed the stereological measurements on H&E stained thyroid sections as previously reported by Miler et al. (2014). In brief, the measurements were carried out using a newCAST stereological software package (VIS – Visiopharm Integrator System, version 3.2.7.0; Visiopharm; Denmark). Total thyroid volumes (μm^3), as well as the total volume of thyroid tissue phases (epithelium, stroma and colloid; μm^3) were determined using Cavalieri's principle (Gundersen and Jensen, 1987). Thyroid volume (V_{pt}) was then estimated as $\hat{=} a(p) \cdot BA \cdot \sum i = 1 nPi$ where $a(p)$ is the area associated with each sampling point ($208878.02\ \mu m^2$), BA is the block advance representing the mean distance between two consecutively studied sections ($150\ \mu m$; Dorph-Petersen et al., 2001), n is the number of sections studied for each thyroid, and ΣPi is the sum of points hitting a given target. The same sections were used for estimation of total thyroid volumes as well as the volumes of thyroid tissue phases: follicular epithelium, stroma and colloid. The number of analysed thyroids was 5 per group.

Volume density estimation was used to determine the percentage of follicular epithelium, stroma and colloid. Four to five transversal sections from the anterior, central and posterior parts of thyroid (n = 5) were analyzed at objective magnification of x 20. Relative volume densities (V_V) were calculated as the ratio of the number of points hitting each tissue component divided by the number of points hitting the reference space, i.e. analyzed thyroid section: $V_V (\%) = Pp/Pt \times 100$ (Pp, counted points hitting the tissue component, Pt, total of points of the test system hitting reference space). Volume density was calculated for each tissue component per analyzed section. Then, the average value for all analyzed sections was calculated (for each component separately), representing the relative volume density of the epithelium, stroma and colloid.

2.4. Immunohistochemical and immunofluorescent analyses

The representative sections (5 μm thick, on Superfrost Ultra Plus®, Thermo Scientific Menzel-Gläser manufactured slides), from each previously histochemically and stereologically evaluated thyroid, were stained with immunohistochemical (IHC; Miler et al., 2014; Šošić-Jurjević et al., 2016) or immunofluorescent (IF; Šošić-Jurjević et al., 2015) methods, according to previously described procedures.

Shortly, after tissue deparaffinization, we blocked endogenous peroxidase activity by sections incubation with 0.3% hydrogen peroxide in methanol for 15 min. Afterward, thyroid sections were exposed to heat-induced antigen retrieval to demask target antigens. Slides were placed in a container and covered with 0.1 mol/l

Table 1
Effects of citrus flavanones on absolute and relative thyroid weight and absolute thyroid volume in intact (ICON) and sunflower oil-treated (CON) controls, as well as in naringenin- (NAR) and hesperetin (HES) -treated rats.

Groups	Absolute thyroid weight (mg)	Relative thyroid weight (mg x 100/b.w.)	Absolute thyroid volume (mm^3)
ICON	20.2 ± 3.1	2.6 ± 0.6	11.0 ± 2.9
CON	18.9 ± 5.5	2.6 ± 0.4	10.6 ± 1.5
NAR	18.2 ± 2.6	2.4 ± 0.2	10.3 ± 0.8
HES	20.8 ± 1.7	2.7 ± 0.1	9.9 ± 1.6

sodium citrate buffer (pH 6.0), and then heated at 750 W in microwave oven for 10 and 5 min. Reduction of non-specific background staining was achieved by incubation with normal porcine serum (Dakopatts, Glostrup, Denmark) diluted 1:10 for 45 min.

For functional IHC characterization of thyroid tissue (Faggiano et al., 2007; Gérard et al., 2003), the rabbit antisera directed against human thyroglobulin (Tg; Dakopatts, Glostrup, Denmark; 1:500; Catalog No. A0251, Lot No.00010709), the rabbit antisera directed against rat sodium-iodide symporter (NIS; Acris antibodies GmbH, Herford, Germany; 1:1200; Catalog No. EUD4101, Lot No. LN2074A) and the mouse antisera directed against human T$_4$ bound to thyroglobulin (T$_4$-Tg monoclonal antibody; QED Bioscience, San Diego, CA, USA; 1:300; Catalog No. 12102) were applied overnight at 4 °C. It should be noted that: the Tg primary antibody used is appropriate for immunohistochemistry as previously validated by Daco (species reactivity includes cow and pig); the T4-Tg primary antibody used is appropriate for immunohistochemistry (validated by Šošić-Jurjević et al., 2014, 2015) and ELISA as previously validated by QED Bioscience (species reactivity includes mouse); and the NIS primary antibody used is appropriate for immunohistochemistry (frozen and paraffin sections) and immunofluorescence as previously validated by Acris (species reactivity includes rat, human and pig). For the negative control, the primary antibody was substituted with PBS.

For immunodetection of Tg and NIS proteins, swine anti-rabbit IgG-horseradish peroxidase (HRP; Dakopatts, Glostrup, Denmark; 1:100; Code No. P0399, Lot No. 20011615) was applied as a secondary antibody for 1 h. Visualization was performed using Dako liquid diaminobenzidine tetrahydrochloride (DAB) substrate chromogen system (Dako North America, Inc. Carpinteria, CA, USA) at concentrations suggested by the manufacturer. All washes and dilutions were performed using 0.1 mol/l phosphate buffer saline (PBS; pH 7.4). Hematoxylin was used as counterstain and slides were mounted in DPX medium (Sigma-Aldrich, Barcelona, Spain). For the negative control thyroid sections, the primary antibody was substituted with PBS.

For the immunofluorescent analysis of thyroid sections, Alexa Fluor 488 donkey anti-rabbit IgG (Invitrogen Life technologies, CA, USA; 1:200; A21202, Lot: 714258) were applied as a secondary antibody. The sections were then washed in PBS 5 times for 5 min. Afterward, sections were incubated with RNase A (10 μg/ml; Thermo Fisher Scientific Inc., Rockford, IL, USA; 20 min at 37 °C), and nuclei were counterstained with propidium iodide (PI; diluted in 2× saline sodium citrate buffer, SSC, 1:300) for 1.5 min. Sections were washed 3 times for 1 min in 2× SSC buffer and 1 time for 5 min in PBS and cover slipped with Mowiol 4–88 (Sigma-Aldrich Co., St. Louis, MO, USA). Images were obtained using a confocal laser scanning microscope Olympus FV10-ASW (Olympus FLUOVIEW FV1000; Germany). An Ar-ion (488 nm) and HeNe (G; 543 nm) lasers were used for excitation of fluorescence.

2.5. Quantitative analyses of digital immunohistochemistry images

The analyses were performed as previously being reported by Ajdžanović et al. (2016).

Namely, stained percentage color area for DAB immunopositive follicles of Tg was evaluated using Windows based ImageJ (Image J, Version 1.49j) plugin named as IHC profiler according to the previously described procedures (Varghese et al., 2014). For DAB immunopositive follicle analyses, 10 unbiasedly captured images (the Leica light microscopic tool that has already been described; 2088 × 1550 pixels, ×10 objective magnification) *per* thyroid tissue *pe*r animal were analyzed. Measurements of relative intensity of fluorescence (RIF) were determined using the ImageJ software (Image J, Version 1.49j). In brief, thyroid T$_4$-Tg IF-stained follicles were encircled with freeform drawing tool, measuring integrated density (ID) of 50 immune positive follicles *per* thyroid tissue *per* animal. Three other immune negative spots in proximity to IF-stained follicles were also rounded for measurements of mean fluorescence of background readings (MB). RIF was calculated using the formula: RIF = ID − (CA × MB), where CA represents area of selected follicles.

2.6. Hormonal analyses

The serum were separated from trunk blood after decapitation and left at room temperature for 2 h, after which it was stored at −70 °C. The serum levels of TSH and total T$_4$ were measured by the enzyme-linked immunosorbent assay (ELISA) using rat TSH kit (IBL International GmbH, Hamburg, Germany) and T$_4$ kit provided by Cusabio Biotech Co. Ltd (Wuhan, Hubei, China). All samples were assayed in duplicate together in one run with intra-assay coefficient of variation of 8.8% for TSH and <15% for T$_4$.

2.7. Statistical analyses

Statistical analyses of all obtained results were performed using GraphPad Prism v.6 for Windows (San Diego, CA, USA). The data for the experimental groups were firstly tested for normality of distribution with the Kolmogorov–Smirnov test and the equality of variance by Bartlett's test. One-way ANOVA was used for further comparative evaluation, followed by Dunett's *post hoc* test. The effect of citrus flavanone treatments on all examined parameters were evaluated in comparison with the values obtained for CON group. There were no differences between the ICON and CON groups for all measured parameters. A confidence level of $p < 0.05$ was considered statistically significant. The data are presented as the means ± SD.

3. Results

3.1. Thyroid gland weight and total thyroid volume

Results on absolute and relative thyroid weight as well as total thyroid volume after treatment with citrus flavanones are summarized in Table 1. Neither one of the examined parameters changed after NAR and HES administration (Table 1).
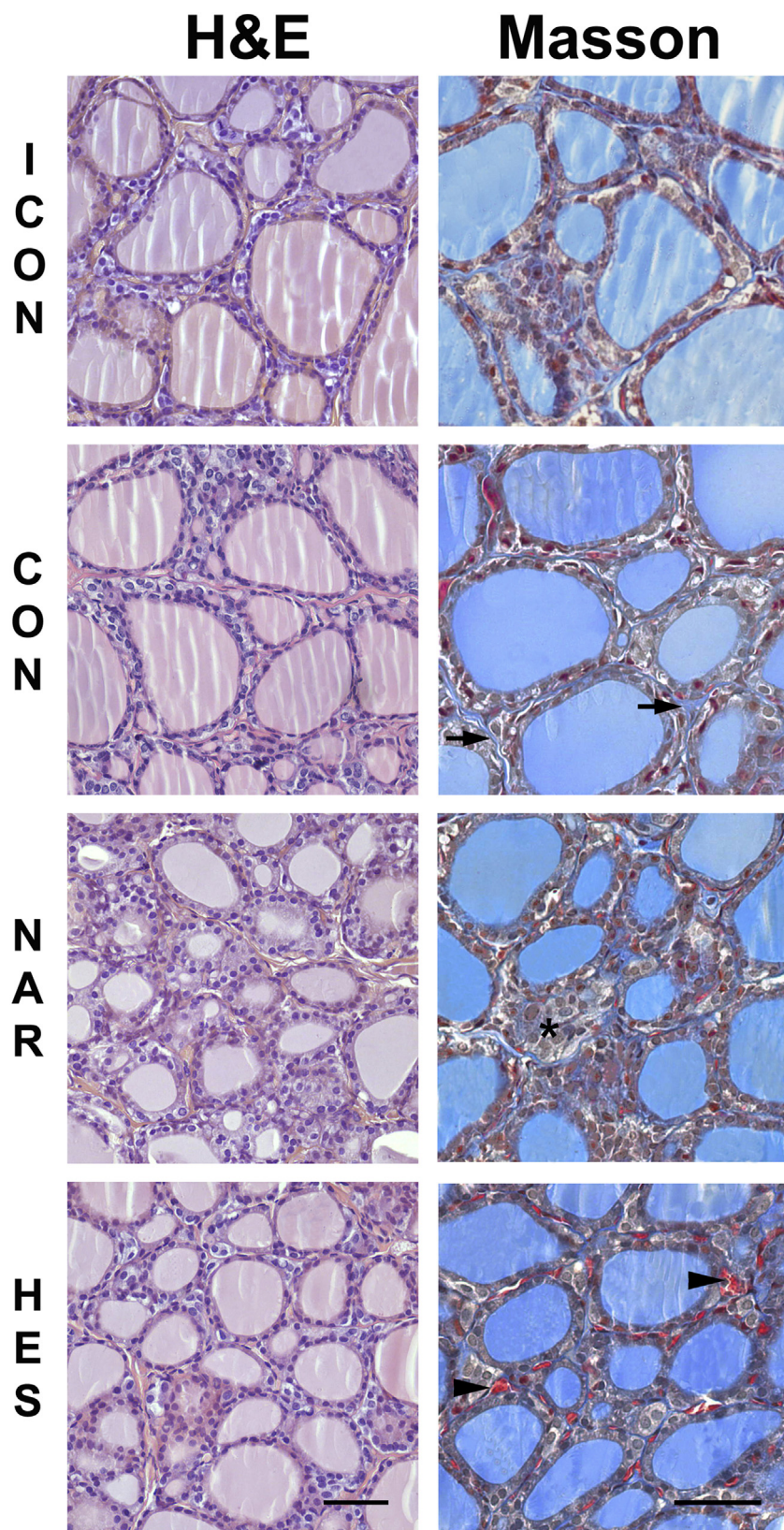
Fig. 1. Representative micrographs of hematoxylin and eosin (H&E) and Masson tricrome stained thyroid sections of intact control (ICON), control sunflower oil-treated (CON), naringenin- (NAR) and hesperetin- (HES) treated rats. Arrows point to connective tissue septa of thyroid stroma; arrowheads point to follicular microvessels and asterisk point on parafollicular cells. 20× magnification, bar = 50 μm.
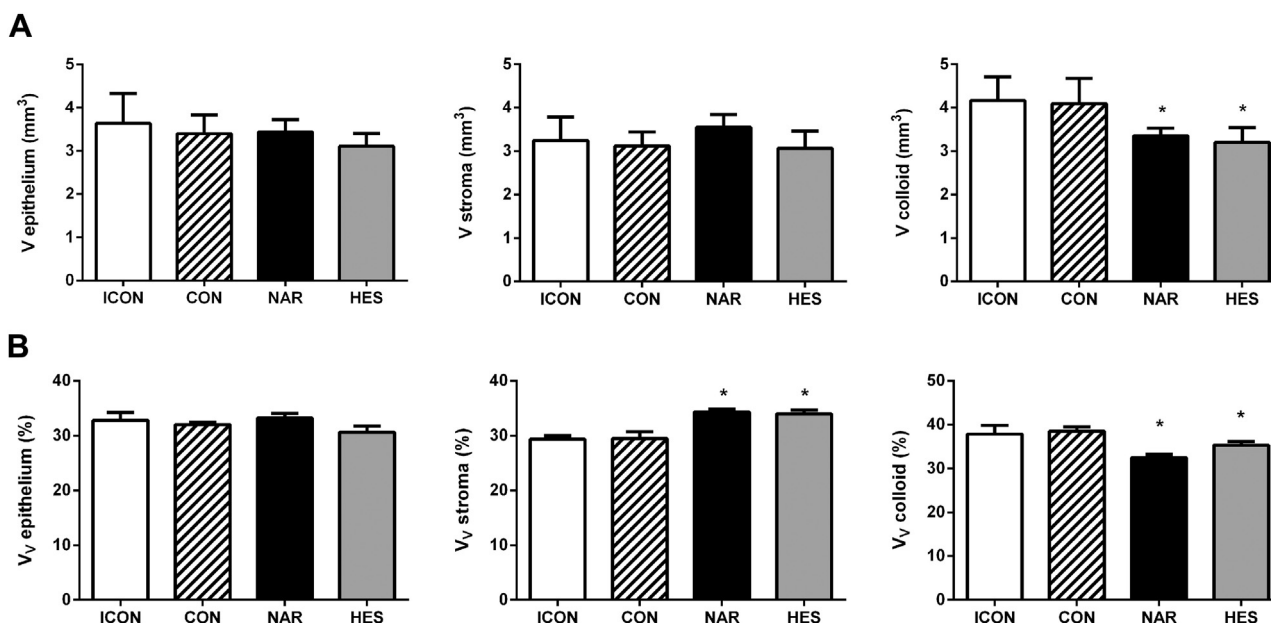
Fig. 2. (A) The absolute volume density (V, mm³) of epithelium, stroma and colloid and (B) relative volume density (Vv; %) of epithelium, stroma, colloid in the thyroids of intact control (ICON), control sunflower oil-treated (CON), naringenin- (NAR) and hesperetin- (HES) treated rats. All of the values presented mean ± SD (n = 5); statistics: one way ANOVA, Dunett's multiple comparison *post hoc* test, *p < 0.05 *versus* CON rats.

3.2. Structural and functional characterization of thyroid tissue

The thyroid parenchyma of both ICON and CON groups was characterized by variability in size of follicles and the amount of luminal colloid. Bigger follicles composed of flattened follicular epithelium and distended colloidal lumen were more numerous in comparison to smaller, more active ones (Fig. 1, H&E staining). Connective tissue of thyroid stroma was regularly distributed throughout the gland (Fig. 1, Masson staining). After NAR or HES treatments, thyroid follicles contained lesser amount of colloid in comparison to the corresponding controls, NAR being more effective in decreasing colloid amount (Fig. 1, H&E staining). The stroma thyroid tissue after flavanone treatments was characterized by increased portion of interfollicular C cells after NAR, and more prominent microvascular blood supply after HES (Fig. 1, Masson staining).

Stereologic analysis demonstrated that in NAR- and HES- treated groups absolute volume of thyroid colloid decreased by 18% and 22% (p < 0.05; Fig. 2A), respectively, in comparison to the values obtained for CON. The relative volume density of colloid decreased by 16% and 9%, (p < 0.05; Fig. 2B), respectively, while the relative volume density of the stroma increased by 16% and 14%, (p < 0.05; Fig. 2B), respectively in comparison to the control values.

In the thyroid of CON animals, strong Tg – immunoreactivity was diffusely distributed throughout the cytoplasm of flattened follicular epithelium, being less intense in the luminal colloid (Fig. 3). Smaller follicles were characterized by strong colloidal Tg-immunopositivity.

After NAR or HES treatments, thyroids had stronger Tg-immunopositivity of the luminal colloid (Fig. 3). Optical density of Tg immunostaining was 11% and 10% (p < 0.05) higher, respectively in comparison to the value obtained for CON group (Fig. 3).

Immunofluorescent analysis of T_4 bound to Tg revealed no (or weak) signal within the most prevalent large follicles of ICON and CON thyroids. However, few small follicles were characterized by a strong IF positivity throughout the whole colloid compartment (Fig. 4). Quantitative IF analysis revealed 29% and 34% (p < 0.05; Fig. 4) higher RIF, respectively in NAR and HES rats, in comparison with the value obtained for CON group (Fig. 4).

NIS- immunopositive follicles were mostly next to each other, thus forming NIS-positive follicular areas within the thyroid tissue of CON group. NIS-immunopositivity was diffusely distributed throughout a cytoplasm of some thyrocytes. However, only few thyrocytes expressed NIS- immunopositivity at their basolateral membranes (Fig. 4).

No significant difference in NIS expression was obtained after treatment with citrus flavanones when compared to the controls (Fig. 5).

3.3. Hormonal analyses

Serum concentration of TSH in ICON and CON groups were 1.88 and 2.01 ng/ml (Fig. 6), respectively. TSH concentration increased by 32% (p < 0.05; Fig. 6) only after NAR in comparison with the control values obtained for CON. In both NAR and HES group T_4 level remain unchanged in comparison with the control values (Fig. 6).

4. Discussion

In the present study we showed that citrus flavanones mildly interfered with pituitary-thyroid axis in 24-month-old rats. Both flavanones decreased thyroid colloidal volume, which point to mild depletion of thyroid hormone stores. However, stronger IHC and IF expression of thyroid-specific proteins Tg and T_4-Tg, are in line with preserved capacity of the thyroid to compensate the adverse effects of flavanones. NAR induced more prominent changes of the thyroid tissue than HES and significantly elevated serum TSH concentration.

Daily intake of flavanone from food in humans is in range 2.7–78 mg (Chanet et al., 2012). In our experiment we used the dose of flavanone aglycones that can be nutritionally achieved by consumption of 0.2–1 l of citrus juices (Chanet et al., 2012). Based on allosteric calculations (West and Brown, 2005), the applied dose of flavanone, 15 mg/kg b.w., corresponds to 4.4 mg/kg b.w. in humans. We showed that the applied dose beneficially affected hepatic antioxidant defense system and phospholipid composition in old rats (Miler et al., 2016), as well as membrane fluidity of human erythrocytes (Ajdžanović et al., 2015).
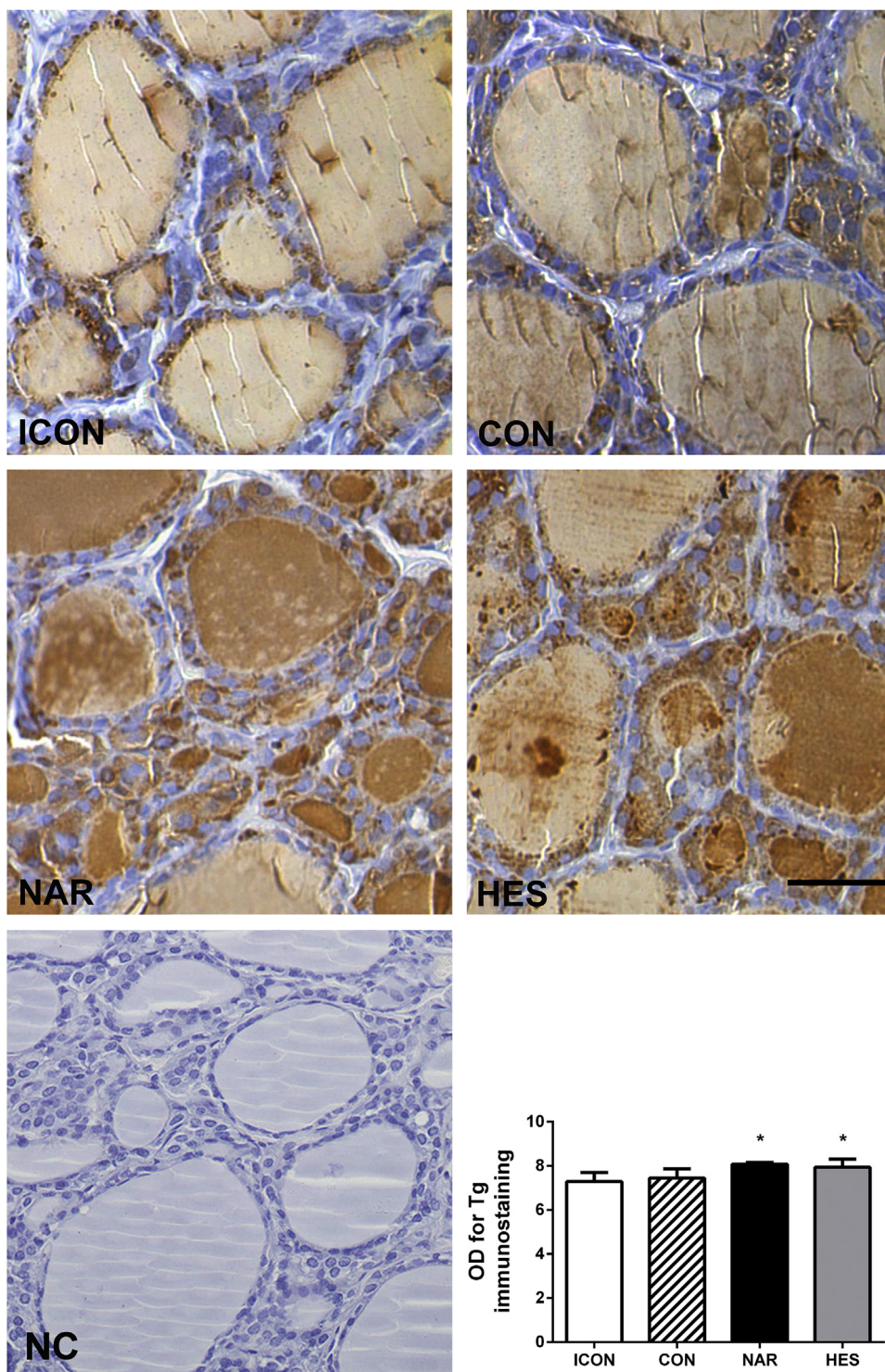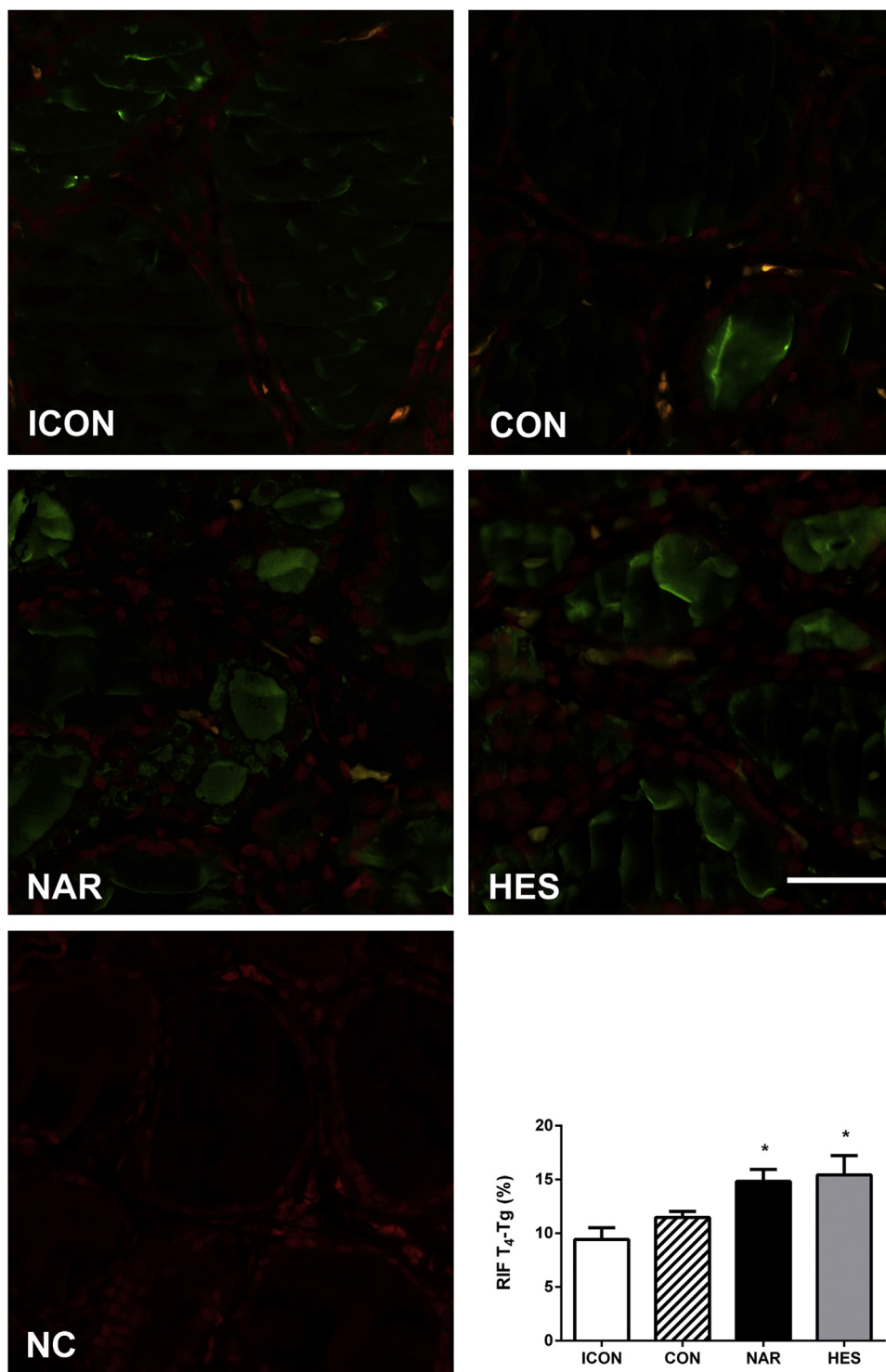
Fig. 3. Representative micrographs of Tg immunopositivity in thyroid gland of intact control (ICON), control sunflower oil-treated (CON), naringenin- (NAR) and hesperetin- (HES) treated rats. Negative control micrograph (NC). $40\times$ magnification, bar = 25 μm. The values for optical density (OD) for Tg are presented mean $\pm$ SD (n = 6); statistics: one way ANOVA, Dunett's multiple comparison *post hoc* test, *p < 0.05 *versus* CON rats.

In comparison to CON animals, thyroid weights and absolute volumes have not been changed after flavanone administrations. In addition, we did not observe tissue hypertrophy or immune cell infiltrations, which indicate no tissue injury. However, treatments with different types of flavonoids, such is vitexin from millet (Mennen et al., 2005) or soy isoflavones in combination with iodine deficiency (Hirose et al., 2001) increase thyroid weight, and could later, after prolonged period of time, lead to development of goiter, autoimmunity and/or cancer (Boelaert, 2013; Vitale et al., 2013).

Histological analyses of the thyroids revealed moderate colloid depletion and stroma increment after NAR- and HES-treatment. These structural changes indicate mild, probably TSH-stimulated changes in TH economy, in line with our previous results with the effects of soy flavonoids (Šosić-Jurjević et al., 2010). Stroma volume increment might be due to a better blood supply and the expansion
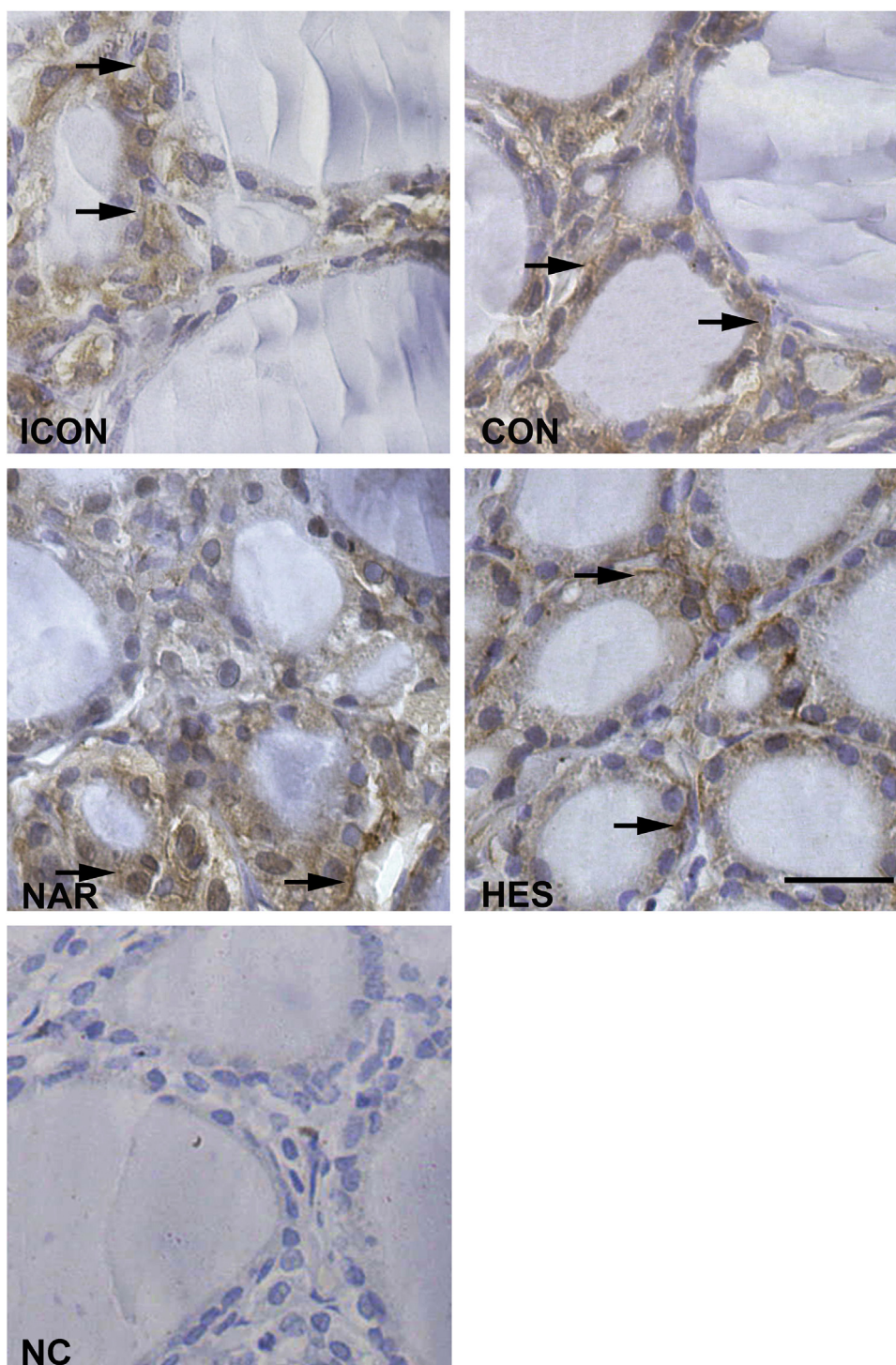
Fig. 4. Representative micrographs of T_4-Tg immunopositivity in thyroid gland of intact control (ICON), control sunflower oil-treated (CON), naringenin- (NAR) and hesperetin- (HES) treated rats. Negative control micrograph (NC). 40× magnification, bar = 25 μm. The values for relative intensity of T_4-Tg immunofluorescence (RIF) are presented mean ± SD (n = 6); statistics: one way ANOVA, Dunett's multiple comparison *post hoc* test, *p < 0.05 *versus* CON rats.

of microcirculation around active follicles. The improved blood supply of angiofollicular units was noticed after TSH stimulation (Colin et al., 2013; Šošić-Jurjević et al., 2015).

IHC characterization of thyroid-specific proteins revealed stronger Tg and T_4-Tg signal within the luminal colloid. NIS expression in follicular epithelium remained unchanged after both treatments. Increase in Tg after flavanone treatments is important, since accumulation of Tg occurs only if some critical amount

of iodine is organified (Gerber et al., 1981). NAR was shown to potently inhibit TPO activity *in vitro* (Divi and Doerge, 1996). However flavonoid rutin, also reported to inhibit TPO activity *in vitro*, but to a lesser extent (Divi and Doerge, 1996), had stimulatory effect on TPO and on the iodide uptake when applied *in vivo* (Lima Gonçalves et al., 2013). In addition, soy isoflavones, which strongly inhibited TPO activity both *in vitro* and *in vivo*, did not affect serum TSH or

Fig. 5. Representative micrographs of NIS immunopositivity in thyroid gland of intact control (ICON), control sunflower oil-treated (CON), naringenin- (NAR) and hesperetin-(HES) treated rats. Negative control micrograph (NC). $40\times$ magnification, bar = 25 μm.

TH hormone concentrations in young adult rats (Chang and Doerge, 2000).

Stronger T_4-Tg RIF after HES in comparison to NAR was expected, keeping in mind all obtained results, and indicate higher inhibitory effect of NAR on TPO activity and TH synthesis. The obtained result, together with unchanged concentration of T_4 in serum indicates compensatory increase and *de novo* synthesis of T_4 by thyroid parenchyma after treatment with flavanones.

TSH level increased only after NAR treatment, even slight increment (but not statistically significant) of TSH after HES was also

evident. Despite the fact that serum T_4 remained unaltered after both flavanone treatments, we cannot exclude possibility of lesser systemic and/or local pituitary T_3 production. Naringin and hesperidin, precursors of flavanone aglycones, were shown to inhibit hepatic deiodinase type 1 enzyme activity in hyperthyroid rats (Panda and Kar, 2014). It seems reasonable to believe that local Dio 1 and 2 activities, already decreased in the pituitary of elderly (Corrêa Da Costa et al., 2001), might be further decreased upon flavanone treatment. This change might induce local hypothyroidism, manifested as elevated TSH secretion after NAR treatment. In con-
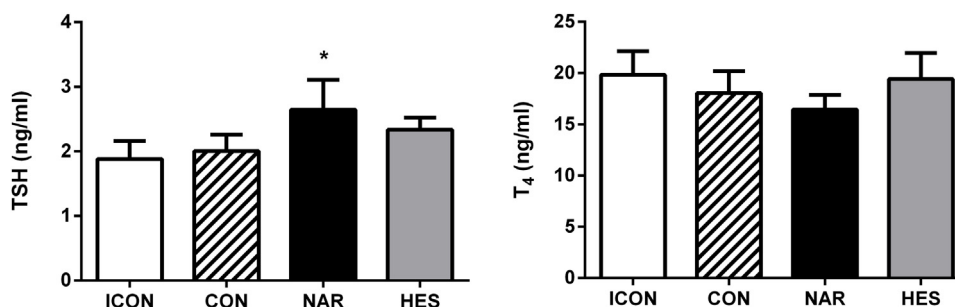
Fig. 6. Serum level of TSH (ng/ml) and T_4 (ng/ml) in intact control (ICON), control sunflower oil-treated (CON), naringenin- (NAR) and hesperetin- (HES) treated rats. All of the values presented mean ± SD (n = 6); statistics: one way ANOVA, Dunett's multiple comparison *post hoc* test, *p < 0.05 *versus* CON rats.

trast to rodents (Cizza et al., 1995; Reymond et al., 1992), circulatory TSH shifts to higher concentrations with advanced age even in population of healthy elderly (Atzmon et al., 2009). Thus, elevated NAR intake might affect local thyroid hormone availability (van der Heide et al., 2003) and stimulate pituitary TSH production and secretion even more prominently then we obtained in rats.

Some studies indicate that elevated TSH level and normal TH, especially after sixth decade of life are related to longer lifespan (Atzmon et al., 2009). An excessive accumulation of detrimental ROS in the pituitary during aging increase the number of apoptotic cells, particularly those that secrete TSH and GH (Vitale et al., 2013). NAR and HES, as potent antioxidants, could prevent this damage and improve thyrotrops sensitivity toward altered TRH and TH regulation with advancing age (Boelaert, 2013). In addition, flavanones may affect paracrine regulation between different pituitary cell types, which express distinct levels of Dio enzymes and/or TH transporters (Denef, 2008; Liao et al., 2011).

In conclusion, NAR elevated serum TSH in old-aged males, thus being more potent than HES in altering pituitary-thyroid axis. However, changes in thyroid structure, namely moderate decrease in colloid volume and stronger IHC Tg and T_4-Tg expressions after both treatments, indicate preserved compensatory mechanism of the gland to maintain T_4 production in old-aged males.

Funding

Acknowledgments

References

Ajdžanović, V., Jakovljević, V., Milenković, D., Konić-Ristić, A., Živanović, J., Jarić, I., Milošević, V., 2015. Positive effects of naringenin on near-surface membrane fluidity in human erythrocytes. Acta Physiol. Hung. 102, 131–136, http://dx. doi.org/10.1556/036.102.2015.2.3.

Ajdžanović, V., Jarić, I., Miler, M., Filipović, B., Šošić-Jurjević, B., Ristić, N., Milenkovic, D., Milošević, V., 2017. Diosgenin-caused changes of the adrenal gland histological parameters in a rat model of the menopause. Acta Histochem. 119, 48–56, http://dx.doi.org/10.1016/j.acthis.2016.11.006.

Ajdžanović, V.Z., Jarić, I.M., Živanović, J.B., Filipović, B.R., Šošić-Jurjević, B.T., Ristić, N.M., Stanković, S.D., Milošević, V.L., 2016. Histological parameters of the adrenal cortex after testosterone application in a rat model of the andropause. Histol. Histopathol. 31, 1209–1220, http://dx.doi.org/10.14670/HH-11-749.

Atzmon, G., Barzilai, N., Hollowell, J.G., Surks, M.I., Gabriely, I., 2009. Extreme Longevity is associated with increased serum thyrotropin. J. Clin. Endocrinol. Metab. 94, 1251–1254, http://dx.doi.org/10.1210/jc.2008-2325.

Boelaert, K., 2013. Thyroid dysfunction in the elderly. Nat. Rev. Endocrinol. 9, 194–204.

Bowers, J., Terrien, J., Clerget-Froidevaux, M.S., Gothie, J.D., Rozing, M.P., Westendorp, R.G.J., Van Heemst, D., Demeneix, B.A., 2013. Thyroid hormone signaling and homeostasis during aging. Endocr. Rev. 34, 556–589, http://dx. doi.org/10.1210/er.2012-1056.

Cavia-Saiz, M., Busto, M.D., Pilar-Izquierdo, M.C., Ortega, N., Perez-Mateos, M., Muñiz, P., 2010. Antioxidant properties, radical scavenging activity and biomolecule protection capacity of flavonoid naringenin and its glycoside naringin: a comparative study. J. Sci. Food Agric. 90, 1238–1244, http://dx.doi. org/10.1002/jsfa.3959.

Chahal, H., Drake, W., 2007. The endocrine system and ageing. J. Pathol. 211, 173–180, http://dx.doi.org/10.1002/path.

Chanet, A., Milenkovic, D., Manach, C., Mazur, A., Morand, C., 2012. Citrus flavanones: what is their role in cardiovascular protection? J. Agric. Food Chem. 60, 8809–8822, http://dx.doi.org/10.1021/jf300669s.

Chang, H.C., Doerge, D.R., 2000. Dietary genistein inactivates rat thyroid peroxidase in vivo without an apparent hypothyroid effect. Toxicol. Appl. Pharmacol. 168, 244–252, http://dx.doi.org/10.1006/taap.2000.9019.

Cizza, G., Gold, P.W., Chrousos, G.P., 1995. Aging is associated in the 344/N fischer rat with decreased stress responsivity of central and peripheral catecholaminergic systems and impairment of the hypothalamic-pituitary-adrenal axis. Ann. N. Y. Acad. Sci. 771, 491–511, http:// dx.doi.org/10.1111/j.1749-6632.1995.tb44705.x.

Cody, V., Koehrle, J., Auf'mkolk, M., Hesch, R.D., 1986. Structure-activity relationships of flavonoid deiodinase inhibitors and enzyme active-site models. Prog. Clin. Biol. Res. 213, 373–382.

Colin, I.M., Denef, J.-F., Lengelé, B., Many, M.-C., Gérard, A.-C., 2013. Recent insights into the cell biology of thyroid angiofollicular units. Endocr. Rev. 34, 209–238, http://dx.doi.org/10.1210/er.2012-1015.

Corrêa Da Costa, V.M., Moreira, D.G., Rosenthal, D., 2001. Thyroid function and aging: gender-related differences. J. Endocrinol. 171, 193–198.

Denef, C., 2008. Paracrinicity: the story of 30 years of cellular pituitary crosstalk. J. Neuroendocrinol. 20, 1–70, http://dx.doi.org/10.1111/j.1365-2826.2007. 01616.x.

Divi, R.L., Doerge, D.R., 1996. Inhibition of thyroid peroxidase by dietary flavonoids. Chem. Res. Toxicol. 9, 16–23, http://dx.doi.org/10.1021/tx950076m.

Donda, A., Reymond, F., Rey, F., Lemarchand-Béraud, T., 1990. Sex steroids modulate the pituitary parameters involved in the regulation of TSH secretion in the rat. Acta Endocrinol. (Copenh). 122, 577–584, http://dx.doi.org/10.1530/ ACTA.0.1220577.

Dorph-Petersen, K.-A., Nyengaard, J.R., Gundersen, H.J.G., 2001. Tissue shrinkage and unbiased stereological estimation of particle number and size*. J. Microsc. 204, 232–246, http://dx.doi.org/10.1046/j.1365-2818.2001.00958.x.

Erlund, I., 2004. Review of the flavonoids quercetin, hesperetin, and naringenin. Dietary sources, bioactivities, bioavailability, and epidemiology. Nutr. Res. 24, 851–874, http://dx.doi.org/10.1016/j.nutres.2004.07.005.

Faggiano, A., Caillou, B., Lacroix, L., Talbot, M., Filetti, S., Bidart, J., Schlumberger, M., 2007. Functional characterization of human thyroid tissue with immunohistochemistry. Thyroid 17, 203–211, http://dx.doi.org/10.1089/thy. 2006.0174.

Gérard, A.-C., Daumerie, C., Mestdagh, C., Gohy, S., de Burbure, C., Costagliola, S., Miot, F., Nollevaux, M.-C., Denef, J.-F., Rahier, J., Franc, B., De Vijlder, J.J.M., Colin, I.M., Many, M.-C., 2003. Correlation between the loss of thyroglobulin iodination and the expression of thyroid-Specific proteins involved in iodine metabolism in thyroid carcinomas. J. Clin. Endocrinol. Metab. 88, 4977–4983, http://dx.doi.org/10.1210/jc.2003-030586.

Galluzzo, P., Ascenzi, P., Bulzomi, P., Marino, M., 2008. The nutritional flavanone naringenin triggers antiestrogenic effects by regulating estrogen receptor α-palmitoylation. Endocrinology 149, 2567–2575, http://dx.doi.org/10.1210/ en.2007-1173.

Gerber, H., Studer, H., Conti, A., Engler, H., Kohler, H., Haeberli, A., 1981. Reaccumulation of thyroglobulin and colloid in rat and mouse thyroid follicles

during intense thyrotropin stimulation. A clue to the pathogenesis of colloid goiters. J. Clin. Invest. 68, 1338–1347, http://dx.doi.org/10.1172/JCI110381.

Gundersen, H.J., Jensen, E.B., 1987. The efficiency of systematic sampling in stereology and its prediction. J. Microsc. 147, 229–263.

Hirose, M., Nishikawa, A., Shibutani, M., Mitsumori, K., 2001. Environmental agents, endocrine disrupting chemicals and rat thyroid carcinogenesis. J. Toxicol. Pathol. 14, 71–77, http://dx.doi.org/10.1293/tox.14.71.

Kim, E.S., Lim, D.J., Baek, K.H., Lee, J.M., Kim, M.K., Kwon, H.S., Song, K.H., Kang, M.I., Cha, B.Y., Lee, K.W., Son, H.Y., 2010. Thyroglobulin antibody is associated with increased cancer risk in thyroid nodules. Thyroid 20, 885–891, http://dx.doi.org/10.1089/thy.2009.0384.

Liao, X.-H., Di Cosmo, C., Dumitrescu, A.M., Hernandez, A., Van Sande, J., St. Germain, D.L., Weiss, R.E., Galton, V.A., Refetoff, S., 2011. Distinct roles of deiodinases on the phenotype of mct8 defect: a comparison of eight different mouse genotypes. Endocrinology 152, 1180–1191, http://dx.doi.org/10.1210/en.2010-0900.

Lima Gonçalves, C.F., de Souza dos Santos, M.C., Ginabreda, M.G., Soares Fortunato, R., Pires de Carvalho, D., Freitas Ferreira, A.C., 2013. Flavonoid rutin increases thyroid iodide uptake in rats. PLoS One 8 (1), http://dx.doi.org/10.1371/journal.pone.0073908.

Mennen, L.I., Walker, R., Bennetau-Pelissero, C., Scalbert, A., 2005. Risks and safety of polyphenol consumption. Am. J. Clin. Nutr. 81, 326–329, 81/1/326S [pii].

Miler, M., Šošić-Jurjević, B., Nestorović, N., Ristić, N., Medigović, I., Savin, S., Milošević, V., 2014. Morphological and functional changes in pituitary-thyroid axis following prolonged exposure of female rats to constant light. J. Morphol. 275, http://dx.doi.org/10.1002/jmor.20293.

Miler, M., Živanović, J., Ajdžanović, V., Oreščanin-Dušić, Z., Milenković, D., Konić-Ristić, A., Blagojević, D., Milošević, V., Šošić-Jurjević, B., 2016. Citrus flavanones naringenin and hesperetin improve antioxidant status and membrane lipid compositions in the liver of old-aged Wistar rats. Exp. Gerontol. 84, 49–60, http://dx.doi.org/10.1016/j.exger.2016.08.014.

Morganti, S., Ceda, G.P., Saccani, M., Milli, B., Ugolotti, D., Prampolini, R., Maggio, M., Valenti, G., Ceresini, G., 2005. Thyroid disease in the elderly: sex-related differences in clinical expression. J. Endocrinol. Invest. 28, 101–104.

Panda, S., Kar, A., 2014. Antithyroid effects of naringin, hesperidin and rutin in L-T4 induced hyperthyroid rats: possible mediation through 5(DI activity. Pharmacol. Rep. 66, 1092–1099, http://dx.doi.org/10.1016/j.pharep.2014.07.002.

Reymond, F., Dénéréaz, N., Lemarchand-Béraud, T., 1992. Thyrotropin action is impaired in the thyroid gland of old rats. Acta Endocrinol. (Copenh). 126, 55–63, http://dx.doi.org/10.1530/ACTA.0.1260055.

Schmutzler, C., Hamann, I., Hofmann, P.J., Kovacs, G., Stemmler, L., Mentrup, B., Schomburg, L., Ambrugger, P., Grüters, A., Seidlova-Wuttke, D., Jarry, H., Wuttke, W., Köhrle, J., 2004. Endocrine active compounds affect thyrotropin and thyroid hormone levels in serum as well as endpoints of thyroid hormone action in liver, heart and kidney. Toxicology 205, 95–102, http://dx.doi.org/10.1016/j.tox.2004.06.041.

Šošić-Jurjević, B., Filipović, B., Wirth, E.K., Živanović, J., Radulović, N., Janković, S., Milošević, V., Köhrle, J., 2014. Soy isoflavones interfere with thyroid hormone homeostasis in orchidectomized middle-aged rats. Toxicol. Appl. Pharmacol. 278, 124–134, http://dx.doi.org/10.1016/j.taap.2014.04.018.

Šošić-Jurjević, B., Filipović, B., Renko, K., Miler, M., Trifunović, S., Ajdžanovič, V., Köhrle, J., Milošević, V., 2015. Testosterone and estradiol treatments differently affect pituitary-thyroid axis and liver deiodinase 1 activity in orchidectomized middle-aged rats. Exp. Gerontol. 72, 85–98, http://dx.doi.org/10.1016/j.exger.2015.09.010.

Šošić-Jurjević, B., Ajdžanović, V., Filipović, B., Trifunović, S., Jarić, I., Ristić, N., Milošević, V., 2016. Functional morphology of pituitary -thyroid and -adrenocortical axes in middle-aged male rats treated with Vitex agnus castus essential oil. Acta Histochem. 118, 736–745, http://dx.doi.org/10.1016/j.acthis.2016.07.007.

Šošić-Jurjević, B., Filipović, B., Ajdzanović, V., Savin, S., Nestorović, N., Milosević, V., Sekulić, M., 2010. Suppressive effects of genistein and daidzein on pituitary-thyroid axis in orchidectomized middle-aged rats. Biol. Med. 235, 590–598, http://dx.doi.org/10.1258/ebm.2009.009279.

Surks, M.I., Hollowell, J.G., 2007. Age-specific distribution of serum thyrotropin and antithyroid antibodies in the U.S. population: implications for the prevalence of subclinical hypothyroidism. J. Clin. Endocrinol. Metab. 92, 4575–4582, http://dx.doi.org/10.1210/jc.2007-1499.

Varghese, F., Bukhari, A.B., Malhotra, R., De, A., 2014. IHC profiler: an open source plugin for the quantitative evaluation and automated scoring of immunohistochemistry images of human tissue samples. PLoS One 9, e96801, http://dx.doi.org/10.1371/journal.pone.0096801.

Vitale, G., Salvioli, S., Franceschi, C., 2013. Oxidative stress and the ageing endocrine system. Nat. Rev. Endocrinol. 9, 228–240, http://dx.doi.org/10.1038/nrendo.2013.29.

van der Heide, D., Kastelijn, J., Schröder-van der Elst, J.P., 2003. Flavonoids and thyroid disease. Biofactors 19, 113–119.